Translational Oncology 26 (2022) 101549

Contents lists available at ScienceDirect

Translational Oncology

journal homepage: www.elsevier.com/locate/tranon

Original Research

Thioridazine combined with carboplatin results in synergistic inhibition of triple negative breast cancer by targeting cancer stem cells

Yi Wang [a,1], Leiming Xia [b,1], Jing Lin [a,1], Li Gong [c], Yang Xia [d], Yang Xu [a], Liu Liu [a], Jian Bao [a], Congshu Zhang [a], Yuqing Chai [a], Hongxia Li [a,*]

[a] Department of Oncology, The First People's Hospital of Hefei/The Third Affiliated Hospital of Anhui Medical University, Hefei 230061, Anhui, PR China
[b] Department of Hematopathology, The Fourth Affiliated Hospital of Anhui Medical University, Hefei 230002, Anhui, PR China
[c] Department of Oncology, East District of First Affiliated Hospital of Anhui Medical University, Hefei 231600, Anhui, PR China
[d] Department of Oncology, Taizhou People's Hospital/The Affiliated Taizhou People's Hospital of Nanjing Medical University, Taizhou 225300, Jiangsu, PR China

ARTICLE INFO

Keywords:
Cancer stem cells
Carboplatin
Synergistic inhibition
Lung metastasis
Thioridazine

ABSTRACT

Cancer stem cells (CSCs) in triple-negative breast cancer (TNBC) are closely related to tumorigenesis and metastasis. Thioridazine (THZ) is a usual phenothiazine antipsychotic drug that can destroy CSCs. We aimed to explore whether THZ could sensitize metastatic TNBC cells, especially the CSCs, to carboplatin (CBP) treatment. Metastatic TNBC cells, 4T1 cells, and tumor-bearing mice were treated with THZ and CBP as monotherapy or combination therapy. MTT, flow cytometry, electron microscopy, immunohistochemistry and western blotting were applied to assess the cell viability, apoptosis, mitochondrial morphology and the relevant protein levels, respectively. Tumor size and lung metastasis under different treatments as well as tumorigenesis of residual tumor cells from each group were monitored. THZ combined with CBP inhibited 4T1 tumor cell proliferation and induced apoptosis by inhibiting the PI3K-AKT-mTOR pathway and activating estrogen receptor stress. THZ also showed strong activity against breast CSCs, THZ combined with CBP significantly destroyed cancer cells, inhibited lung metastasis and relieved the tumor burden; Our data demonstrated that THZ can sensitize TNBC cells to CBP treatment and this combination therapy may provide a bright strategy for TNBC treatment by targeting both cancer cells and CSCs.

Introduction

Triple-negative breast cancer (TNBC) is an most aggressive type of breast cancer (BC) characterized by the absence of estrogen receptor (ER), progesterone receptor, and human epidermal growth factor receptor 2 (HER-2) [1,2]. TNBC is the most fatal subtype of BC with high heterogeneity, aggressive progression, and poor response to current therapy modalities. The high recurrence and frequent metastasis associated with TNBC often result in poor overall survival outcomes [3]. Thus, the exploration of more effective and less toxic approaches is urgently needed for the treatment of TNBC. Cancer stem cells (CSCs) are responsible for initiation, disease progression, tumor recurrence, and metastasis [4]. Our previous studies demonstrated that CSC-targeted therapies could dramatically improve the inhibition of both primary tumors and metastasis [5]. However, few CSC-targeted strategies are currently available for clinical use.

Thioridazine (THZ) is a commonly used antipsychotic drug with acceptable side effects. Moreover, recent work has shown that THZ has an inherent and potent anti-tumor effect via P-glycoprotein reduction [6] and DNA damage [7]. More surprisingly, THZ was recently reported to specifically target breast CSCs (BCSCs), Lang et al. described that although THZ exhibited no effect on MCF-7 cells, it could distinctly destroy MCF-7 CSCs by antagonizing the highly expressed dopamine receptors on MCF-7 CSCs [8, 9]. Nonetheless, whether THZ targets CSCs in TNBC is still not fully understood.

Platinum-based chemotherapies have achieved a high pathological complete remission rate in patients with TNBC [10]. Data from a phase III trial demonstrated that carboplatin (CBP) exerted similar effectiveness and less toxicity than docetaxel in 376 metastatic TNBC patients [11]. Clinical trials have reported that platinum-based therapy could induce a significant response in TNBC patients. For example, a CBP plus taxane chemotherapy regimen showed a high pathological complete

* Corresponding author.
E-mail address: lihongxia_dr@163.com (H. Li).
[1] Yi Wang, Leiming Xia and Jing Lin contributed equally and share the first authorship.

https://doi.org/10.1016/j.tranon.2022.101549
Received 26 March 2022; Received in revised form 14 July 2022; Accepted 16 September 2022

response (PCR) in TNBC patients [12]. Moreover, a multivariate analysis indicated that CBP administration resulted in a remarkable improvement in PCR [12–14]. Combination therapy is a mainstay of cancer treatment, and optimal combinations can produce synergistic antitumor responses. Common metastatic animal models for stage IV human TNBC are often constructed with 4T1 cells due to their high tumorigenicity and invasion.

In this study, we investigated the efficacy and mechanism of THZ in combination with carboplatin (CBP) in the suppression of 4T1 cells in vitro and in vivo. We also examined the potential effects of this regimen on $ALDH^{high}$ (aldehyde dehydrogenase) 4T1 CSCs. The phosphorylation levels of components involved in the PI3K/mTOR pathway and the expression of ER stress-related proteins displayed moderate changes under this combination. Our data revealed that THZ produces therapeutic synergism with CBP in TNBC cells by targeting CSCs via PI3K/mTOR and ER stress-mediated apoptosis. These findings suggest that THZ is an efficient drug for TNBC therapy by targeting BCSCs.

Materials and methods

Reagents and antibodies

THZ and CBP were purchased from Sigma-Aldrich (St. Louis, USA). RPMI 1640 medium, fetal bovine serum (FBS), trypsin, streptomycin/penicillin and MTT were obtained from Gibco (Grand Island, USA). Antibodies against β-actin (1:2000), cleaved caspase-3 (1:1000)/caspase-3(1:2000), cleaved caspase-9 (1:1000)/ caspase-9 (1:1000), pro caspase3 (1:1000), pro caspase12 (1:500), BAX (1:2000), Bcl-2 (1:2000), Bcl-xL (1:1000), PTEN (1:1000), PI3K (1:2000)/ phosphorylated (p-)PI3K (1:1000), AKT (1:2000)/ p-AKT (1:1000), mTOR (1:1000)/ p-mTOR (1:500), GRP78 (1:1000), and CHOP (1:1000) were bought from Cell Signaling Technology (Danvers, USA). Antibodies against EGFR (1:500), VEGF (1:200), MMP-2 (1:200) and MMP-9 (1:200) were came from abcam Co. (Cambridge, USA). Horseradish peroxidase enzyme (HRP)-labeled monoclonal antibody was bought from Santa Cruz (Santa Cruz, USA).

Cell culture

The 4T1 cells was obtained from the Cell Bank of the Shanghai Institutes for Biological Sciences (Shanghai, China) and was cultured in the 1640 medium supplemented with 10% FBS, penicillin (100 U/mL), streptomycin (100 μg/mL) at 37°C, 5% CO_2.

Cell viability assay

Cells were seeded in 96-well plates at 2×10^3 cells/well for 24h, and then treated them with THZ, with or without CBP. Cell proliferation was monitored using MTT assay. The absorbance was measured using a microplate reader (Thermo Fisher Scientific, USA) at dual wavelengths of 490 and 630 nm. The mean value of triplicate experiments for each dose was used to represent the cell viability and combination index (CI).

CI calculation

CompuSyn software version 1.0 (ComboSyn Inc., USA) was used to calculate the CIs, which were adopted to evaluate the synergy of both drugs in killing tumor cells. The CIs were interpreted as follows: CI<1: synergism; CI=1: additivity; and CI>1: antagonism.

Mitochondrial damage monitor

Pre-treated 4T1 cells were collected and fixed with 2.5% glutaraldehyde at 4°C for 4 h. Washed three times and then fixed with 1% OsO_4 solution (Alfa, 012103) for 1 h, followed by three more washes. The cells were sequentially dehydrated using an ethanol gradient (HUSHI, 10009218) of 30%, 50%, 70%, 80%, 90%, 95%, and 100% for 15 min, and then in acetone (Sigma-Aldrich, 179124) for 20 min. Then cultured in a mixture (Equal volume of acetone and Spurr resin) for 1 h at room temperature. The treated cells were placed in capsules and heated for 9 h at 70°C . The specimens were dyeing with alkaline lead citrate and uranyl acetate for 15 min. Mitochondrial damage was observed using a transmission electron microscope (Model H-7650, Hitachi, Japan).

Cell apoptosis

Apoptotic cells were determined by an Annexin V/PI double staining apoptosis kit (BD, USA). The 4T1 cells were treated with THZ and/or CBP for 4 h, then digested and collected for the following staining. PBS was used to wash and resuspend the pellets to obtain a single-cell suspension. Then, Annexin-V and PI were added and incubated for 15 min. The apoptotic cells were acquisition using a FACScan flow cytometer (BD FACSCalibur, USA). Data was analyzed using FlowJo Software version VX (Tree Star, Inc., USA).

Western blot

The protein was extracted using RIPA lysis buffer (Cat. No.: HY-K1001; MedChemExpress). Proteins were collected, subjected to SDS-polyacrylamide gel electrophoresis and transfer to PVDF membrane. Bovine serum albumin was used for membrane blocking. Membranes were then incubated with primary antibodies (caspase-3, -9, Bcl-2, Bcl-xL, BAX, PI3K, Akt, and mTOR) overnight at 4°C on a shaker, followed by treated with horseradish peroxidase-conjugated anti-rabbit secondary antibodies (Santa Cruz Biotechnology) for an hour at room temperature with gentle shaking. Protein band signals were detected by ECL reagents (Pierce Biotechnology, USA) and imaged with a ChemiDoc MP system (Bio-Rad Laboratories, Inc.). The band gray intensities were quantified using ImageJ software.

Hematoxylin and eosin (H&E) and immunohistochemistry(IHC) staining

The lungs and tumors were removed and perfused with buffered formalin. The section thickness used for H&E staining is 4μm. For IHC examination, mammary tumors and lung tissues were collected, fixed, embedded, and examined the indicated proteins. Briefly, paraffin-embedded tumor sections were hydrated using graded alcohol and xylene. Quench endogenous peroxidase by treating with 0.3% hydrogen peroxide for 5 min. EGFR, VEGF, MMP-2, and MMP-9 signals were detected. Apoptosis was examined by one step TUNEL apoptosis assay kit (Beyotime Biotechnology, China) according to the manufacturer's protocol. Brown, TUNEL-positive cells were defined as apoptotic cells.

Isolation of $ALDH^{high}$ and $ALDH^{low}$ 4T1 cells

The ALDEFLUOR Kit (Stem Cell Technologies, Canada) was used to isolate the CSCs from the 4T1 cells by ALDH1 staining [5, 15]. In brief, cultured 4T1 cells (1×10^6 cells/mL) from control and treated groups were resuspended and incubated in aldefluor buffer at 37°C. Then cells were washed in aldefluor buffer and maintained at 4°C. The Cell Sorting System and FACSDiva software (version 6.1.2, Dickinson and Company, USA) were used to assess ALDH activity. Fluorescent-activated cell sorting was used to collect cells based on their fluorescence intensity, which corresponds to the level of ALDH activity of the cells. Isolation and culture of cells with $ALDH^{high}$ and $ALDH^{low}$ levels for further study.

Tumorigenicity of $ALDH^{low}$ and $ALDH^{high}$ 4T1 cells

Equal numbers of $ALDH^{low}$ and $ALDH^{high}$ 4T1 cells at three different doses were subcutaneously inoculated into the left and right flanks of 6-8 weeks old BALB/c mice, respectively. Tumor size was measured every three days.

Animal model

All animal experiments were approved by the Animal Welfare Agency of the third Affiliated Hospital of Anhui Medical University (2018-017-01). The mice were obtained from Anhui Medical University and breeding under specific pathogen-free conditions. To evaluate the anti-tumor efficacy of THZ, CBP, and their combination, 1×10^6 4T1 cells were injected into the fat pad of the mice. On day 7, when tumor mass was established, randomly assigned of the mice to different treatment groups. Group I: Control (PBS); Group II: 20 mg/kg THZ through intragastric administration; Group III: 100 mg/kg CBP through intraperitoneal administration; and Group IV: 20 mg/kg intragastric THZ + 100 mg/kg intraperitoneal CBP. The length and width of the tumors were measured two or three times per week. The tumor volumes were calculated by the following formula: volume = ½ × L(length) × W^2(width). Survival was monitored, and survival curves were analyzed using Kaplan-Meier plots. Mice were euthanized with pentobarbital sodium (50 mg/kg, intraperitoneal injection), and the lungs were harvested for enumeration of spontaneous pulmonary metastasis.

To further test the tumor initiation capacity of drug-treated residual tumor cells, we digested tumor tissues harvested from Groups III and IV into single cell suspensions. Then, 0.5×10^6 cells were transplanted into the opposite fat pad of the same mouse. Each group had five replicates. The tumor size and volume were measured.

Statistical analysis

GraphPad Prism 8 (GraphPad Software, USA) was use to analyze all data. Analyze methods such as t-test, one-way ANOVA (followed by Tukey's test), and survival analysis were used and variables are presented as mean ± SD in the figures. P value less than 0.05 indicates statistical significance.

Results

THZ, CBP monotherapy and combination treatment inhibit proliferation of 4T1 cells

To examine whether THZ could enhance the anti-tumor activity of CBP, we tested the proliferation of 4T1 cells subjected to THZ and/or CBP treatment. After incubation for 24 h, the proliferation of 4T1 cells was obviously inhibited by THZ and CBP in a dose-dependent manner, with starting inhibitory concentrations of 20 μM and 0.2 mM, respectively (Fig. 1(a) and (b)). Importantly, we found that the CI of THZ combined with CBP ≤ 1 when THZ was used at the concentrations of 10 μM or 20 μM in combination with 0.8 mM of CBP, indicating the significant synergistic inhibitory effects of the combination of THZ and CBP on 4T1 cells (Fig. 1(c)). Microscope observation of 4T1 cell morphology further confirmed the synergistic inhibitory effects of the combination of

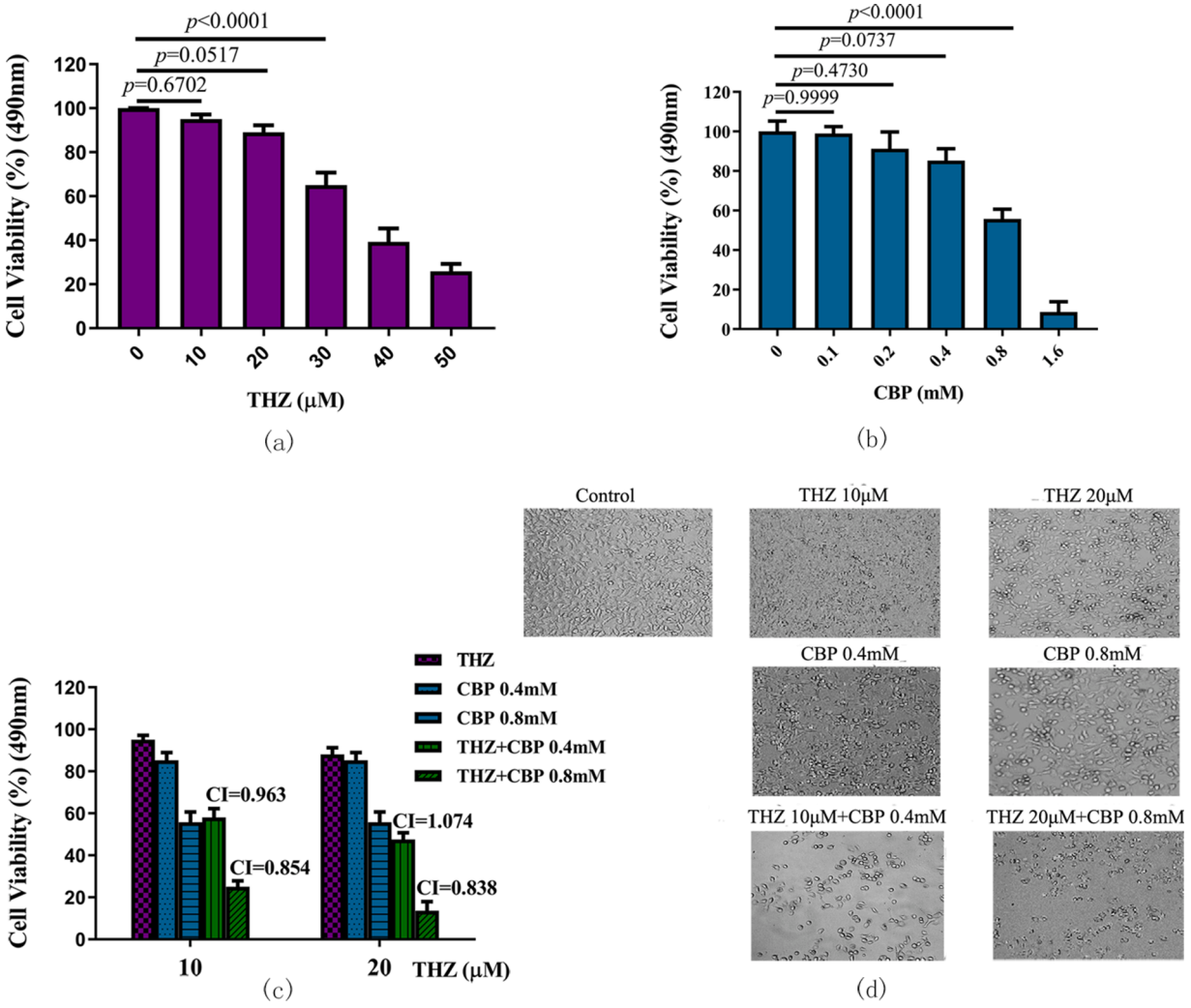

Fig. 1. THZ or CBP monotherapy and combination therapy inhibit proliferation of 4T1 cells. Effect of THZ (a) and CBP (b) on viability of 4T1 cells after 24 hours. (c) The synergistic inhibitory effects of combination therapy on 4T1 cells was observed as CI calculations. (d) Analysis of 4T1 cell density and morphology following exposure to THZ, CBP, or combination therapy for 24 hours. Magnification: 40 x.

20 μM THZ and 0.8 mM CBP (Fig. 1(d)). Therefore, these two dosages were selected for the subsequent studies.

THZ and CBP combination therapy induces apoptosis of 4T1 cells

To further examine the effects of THZ and CBP on 4T1 cells, we examined whether they could affect apoptosis. As shown in Fig. 2(a), impaired mitochondria, such as mitochondrial matrix cavitation and reduction of mitochondrial cristae, were observed in 4T1 cells treated with CBP alone. However, THZ alone did not induce significant mitochondrial damage. In the combination therapy group, cell ultrastructure exhibited typical apoptotic changes, including chromatin condensation and vacuolization, loss of mitochondrial cristae, and high electron-dense matrices.

Subsequently, we evaluated early and late apoptosis in 4T1 cells induced by THZ and CBP monotherapy or combination therapy using Annexin V/PI staining. As shown in Fig. 2(b), monotherapy and combination therapy induced significant apoptosis in the 4T1 cells, and the percentage of apoptotic cells in the THZ only, CBP only, and combination groups were 6.08%, 21.69%, and 60.06%, respectively. Therefore, the combination of THZ and CBP resulted in a more significant increase in apoptosis than THZ or CBP alone (Fig. 2(c)).

To further confirm THZ-induced apoptosis, we first detected the expression of proteins related to the mitochondria-mediated apoptotic pathway, such as cleaved caspase-3/9, Bax, Bcl-xL, and Bcl-2, in THZ- and/or CBP-treated 4T1 cells. THZ and CBP combination therapy significantly upregulation the expression of cleaved caspase-3/9 compared with treated with THZ or CBP alone. In addition, Bax, a pro-apoptotic protein, was upregulated in all groups, especially in the combination group. Furthermore, combination therapy significantly reduced the expression levels of Bcl-xl and Bcl-2, two anti-apoptotic proteins, when compared with THZ or CBP monotherapy (Fig. 2(d) and (e)). Our findings indicated that THZ in combination with CBP could induce apoptosis of 4T1 cells by promoting a caspase-mediated apoptotic pathways.

Apoptosis induced by THZ and/or CBP is regulated by ER stress and the PI3K/AKT/mTOR signaling pathway

To further expound the molecular mechanisms of apoptosis induced by THZ and/or CBP, the expression of endoplasmic reticulum (ER) stress-related proteins were analyzed, including PI3K, PTEN, AKT, and mTOR. As shown below, the expression of p-PI3K, p-AKT, and p-mTOR was decreased in all treatment groups, and the most significant inhibition was observed in the combination therapy group. In contrast, PTEN expression was upregulated (Fig. 3(a) and (b)). In addition, we determined levels of ER stress activation-related proteins, such as GRP78 and CHOP. Both GRP78 and CHOP were upregulated after monotherapy and, especially combination therapy. Furthermore, the levels of cleaved caspase-3 and caspase-12 were also increased in all treatment groups (Fig. 3(c) and (d)). These data indicate that ER stress may be involved in the development of THZ-induced apoptosis via the upregulation of GRP78 and CHOP.

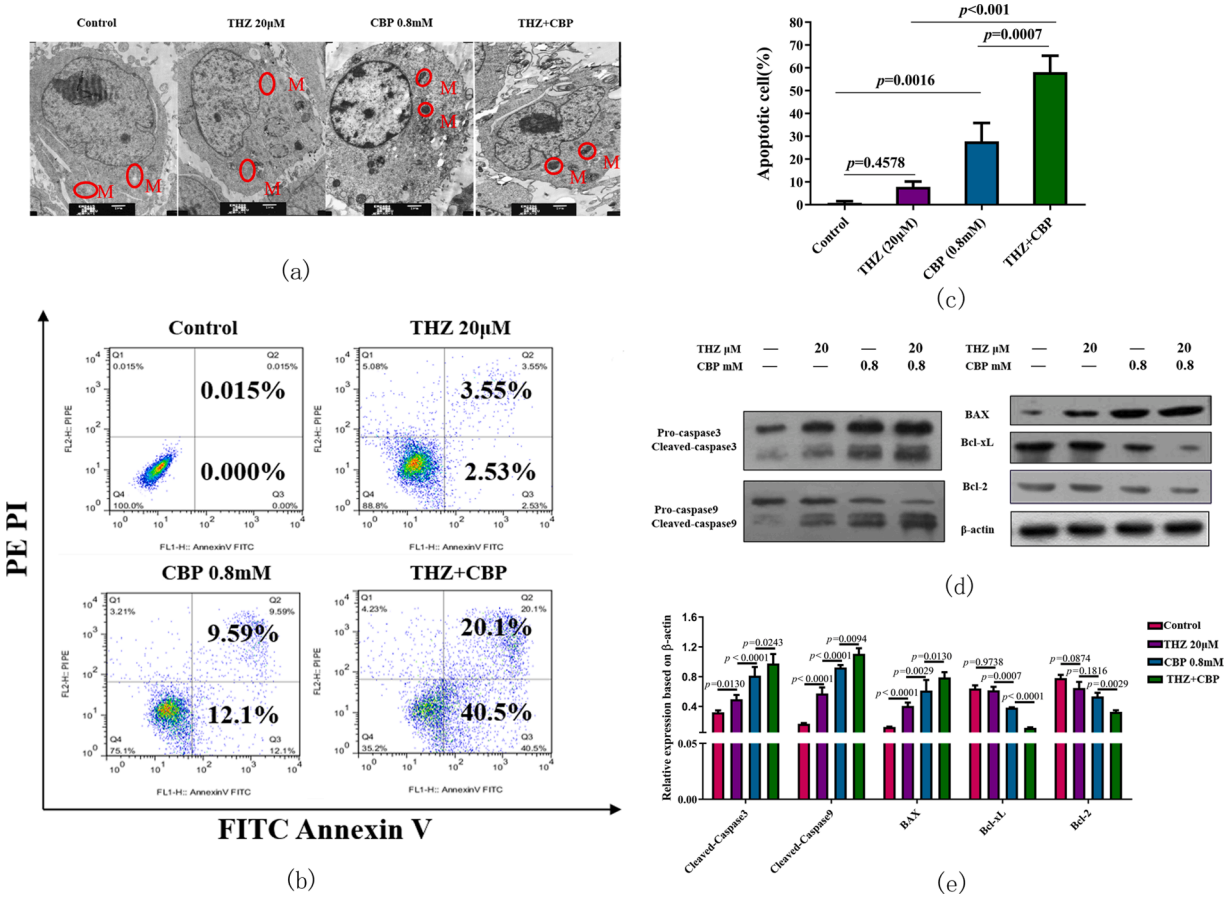

Fig. 2. THZ and CBP combination therapy induced apoptosis of 4T1 cells. (a) Transmission electron microscopy (TEM) was performed to examine THZ + CBP induced apoptosis with obvious swollen mitochondrion (M) and condensed chromatin. Scale bar, 1 μm. (b) Annexin-V and PI staining to show the apoptotic and necrotic cells treated with THZ and CBP for 4 h. (c) Statistical diagram of apoptosis ($n = 3$). (d) Western blot analysis for apoptosis-related protein in 4T1 cells treated with THZ and/or CBP. (e) Quantification of individual protein bands by normalization to β-actin ($n = 3$).

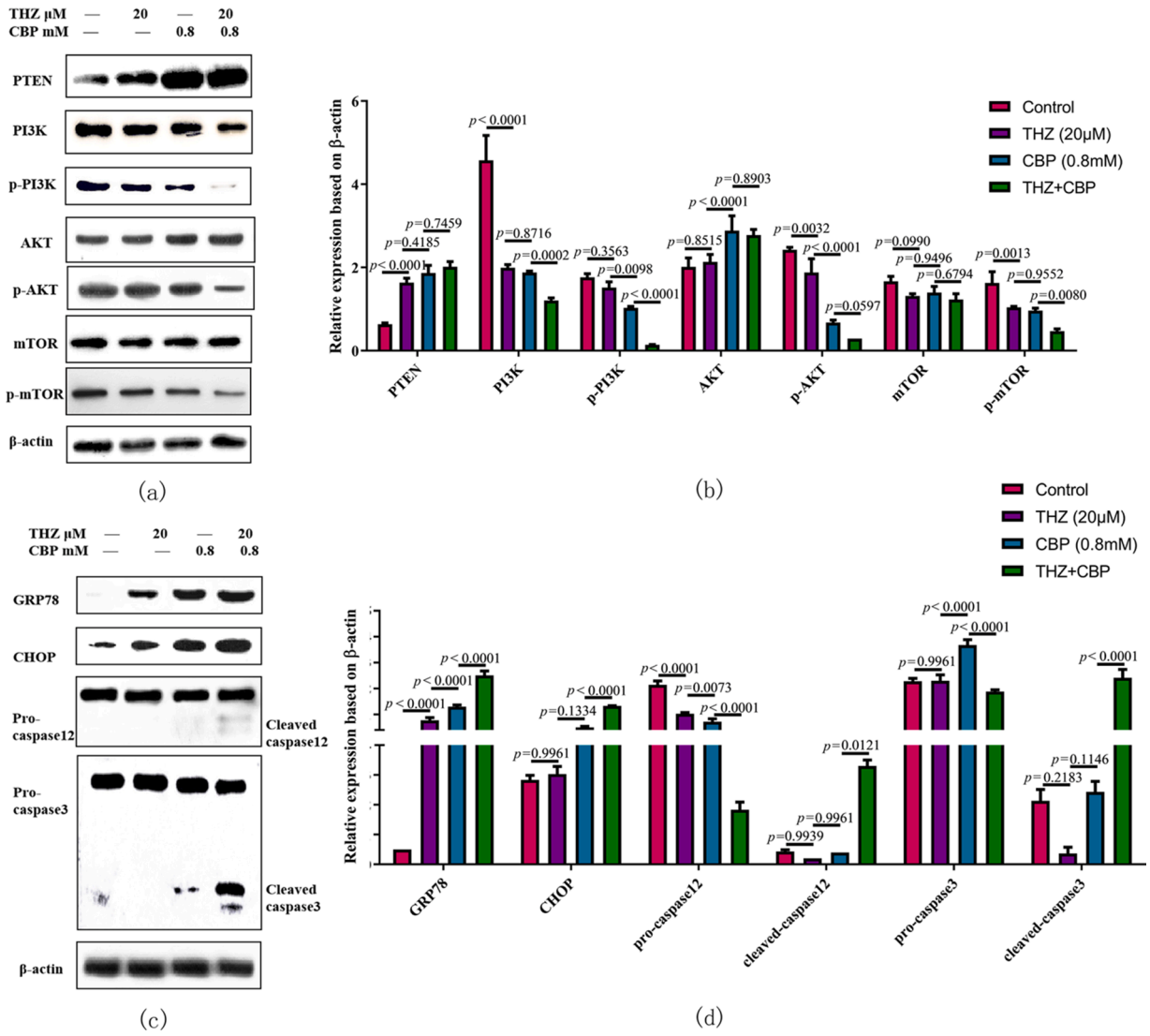

Fig. 3. Inhibition of the PI3K/AKT/mTOR pathway and activation of estrogen receptor (ER) stress are involved in CBP combined with THZ-induced apoptosis. (a, c) Effects of THZ and/or CBP treatment in 4T1 cells on the expression of major components of the PI3K/AKT/mTOR signaling pathway and ER stress-related proteins. (b, d) Quantitative analysis of western blotting ($n = 3$).

Combined THZ and CBP treatment inhibits tumor growth and prolongs animal survival in 4T1 model

To determine the anti-tumor effect of THZ and CBP in vivo, we established BC model in BALB/c mice using 4T1 cells, and divided them into four groups (control, THZ, CBP, and combination). As shown below, CBP alone was effective compared with the control in the 4T1 BALB/c mice. Moreover, combination therapy induced a dramatic reduction in tumor growth, as indicated by tumor weight and volume (Fig. 4(a)-(c)). In addition, H&E staining showed that THZ+CBP-treated tumors contained a large pool of necrotic cells when compared with the monotherapy groups (Fig. 4(d)). Although THZ monotherapy had only a mild effect on tumor apoptosis in the BALB/c mice, we observed that CBP monotherapy or in combination with THZ could induce significant tumor cell apoptosis in 4T1 BALB/c mice, as indicated by increased TUNEL-positive staining in tumor tissues (31±5% and 61±4%, respectively, Fig. 4(e) and (f)). Furthermore, CBP+THZ combination therapy markedly improved the survival of tumor-bearing mice (Fig. 4(g)). Together, these results suggest that combination therapy with THZ and CBP was significantly more effective than monotherapy in the murine breast carcinoma 4T1 BALB/c mice model and could inhibit tumor growth and prolong survival.

THZ enhances CBP suppression on the 4T1 tumor lung metastasis

To explore the potential roles of THZ in enhancing the anti-tumor efficacy of CBP in the 4T1 mouse model, we assessed the lung metastasis ability in each treatment group. Macroscopic observation of lungs harvested from mice treated with the control, THZ, CBP, and THZ+CBP revealed that the total number of tumor nodes was lower in all treatment groups, especially the combination treatment group, than the control (Fig. 5(a)). Furthermore, the average number of harvested tumor nodules was also decreased in the therapy groups, especially the combination treatment group (Fig. 5(b)). Moreover, H&E staining of lung tissues indicated that fewer tumor nodules were found in the combination therapy group than in the monotherapy group (Fig. 5(c)). TUNEL staining results showed that monotherapy with THZ or CBP elicited moderate tumor cell apoptosis in 4T1 BALB/c mice; However, combination therapy with THZ and CBP significantly promoted tumor cell apoptosis in lung tissues (Fig. 5(d)).

Activated vascularization remodeling is important for the establishment of tumor metastasis. Therefore, we investigated the expression of angiogenesis-related proteins, EGFR, VEGF, MMP2, and MMP9, in metastatic lung nodules. IHC staining demonstrated a decreased level of EGFR, VEGF, and MMP2 expression in the treated groups, with a more

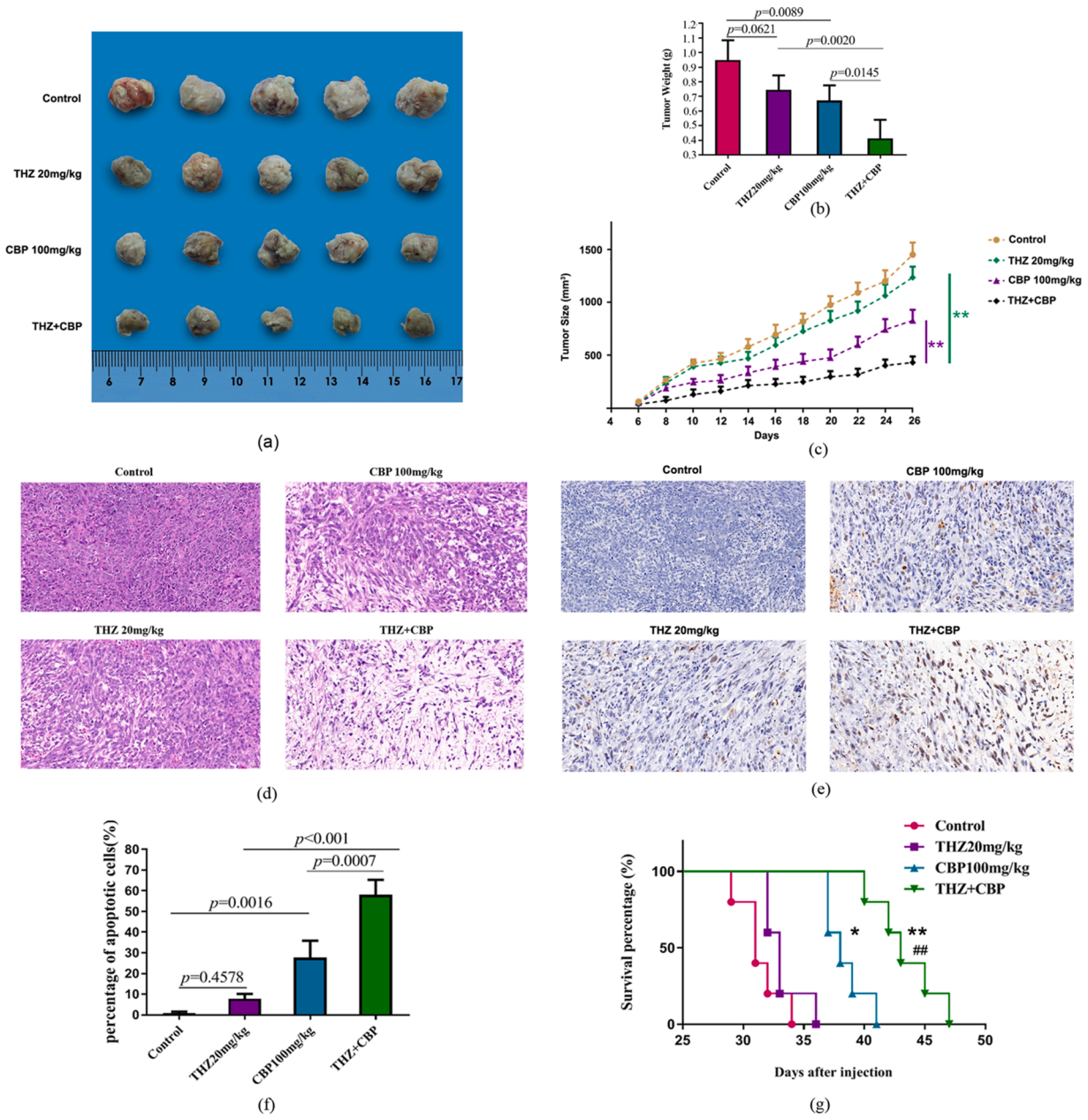

Fig. 4. Systemic administration of CBP and THZ in combination significantly inhibited tumor growth and prolonged survival in the 4T1 mice model. (a) Representative image of tumors from tumor-bearing mice. (b) The average tumor weight ($n = 5$). (c) Statistical analyses of tumor growth after treatment ($n = 5$). (d) Images of H&E staining. (e) Images of TUNEL staining. (f) Percentage of apoptotic cells in different tumor tissues as quantified from TUNEL staining ($n = 3$). (g) Survival analysis of tumor-bearing mice ($n = 5$). Magnification: 400 × . * $P < 0.05$, ** $P < 0.01$, *** $P < 0.001$. $^{\#\#}$ $P < 0.01$. * represents comparison with the control group, $^{\#}$ represents comparison with the CBP group.

significant decrease in the combination therapy group (Fig. 5(e)-(g)). However, MMP9 expression was not affected by THZ monotherapy or combination therapy (Fig. 5(h)). Taken together, our results suggest that THZ could synergistically enhance the anti-tumor efficacy of CBP by suppressing tumor vascularization, and therefore, inhibiting lung metastasis.

THZ and CBP decreases phosphorylation in the PI3K/mTOR pathway and induces ER stress in vivo

To further validate the mechanisms of THZ and CBP observed in 4T1 cells in vitro, we analyzed the PI3K/mTOR pathway and the ER stress-related proteins in the 4T1 mouse model. The expression of phosphorylated molecules in this signaling pathway was significantly reduced after THZ or CBP monotherapy and combination therapy (Fig. 6(a) and (b)). Specifically, combination therapy reduced the phosphorylation of these proteins significantly more than either monotherapy. Furthermore, the upregulated expression of ER stress-related markers indicated that the anti-cancer effect of CBP was notably enhanced by THZ, which was consistent with the in vitro findings. Both GRP78 and CHOP, were upregulated in the THZ or CBP treatment groups, and the combination therapy group demonstrated significantly higher levels of these proteins than THZ or CBP alone (Fig. 6(a) and (b)). In addition, cleaved caspase-3 was found in the CBP alone and THZ +CBP groups (Fig. 6(a) and (b)). In summary, we suggest that inhibition of the PI3K/mTOR pathway and ER stress production enables the mechanism by which THZ promotes the anti-tumor effect of CBP in 4T1 BC.

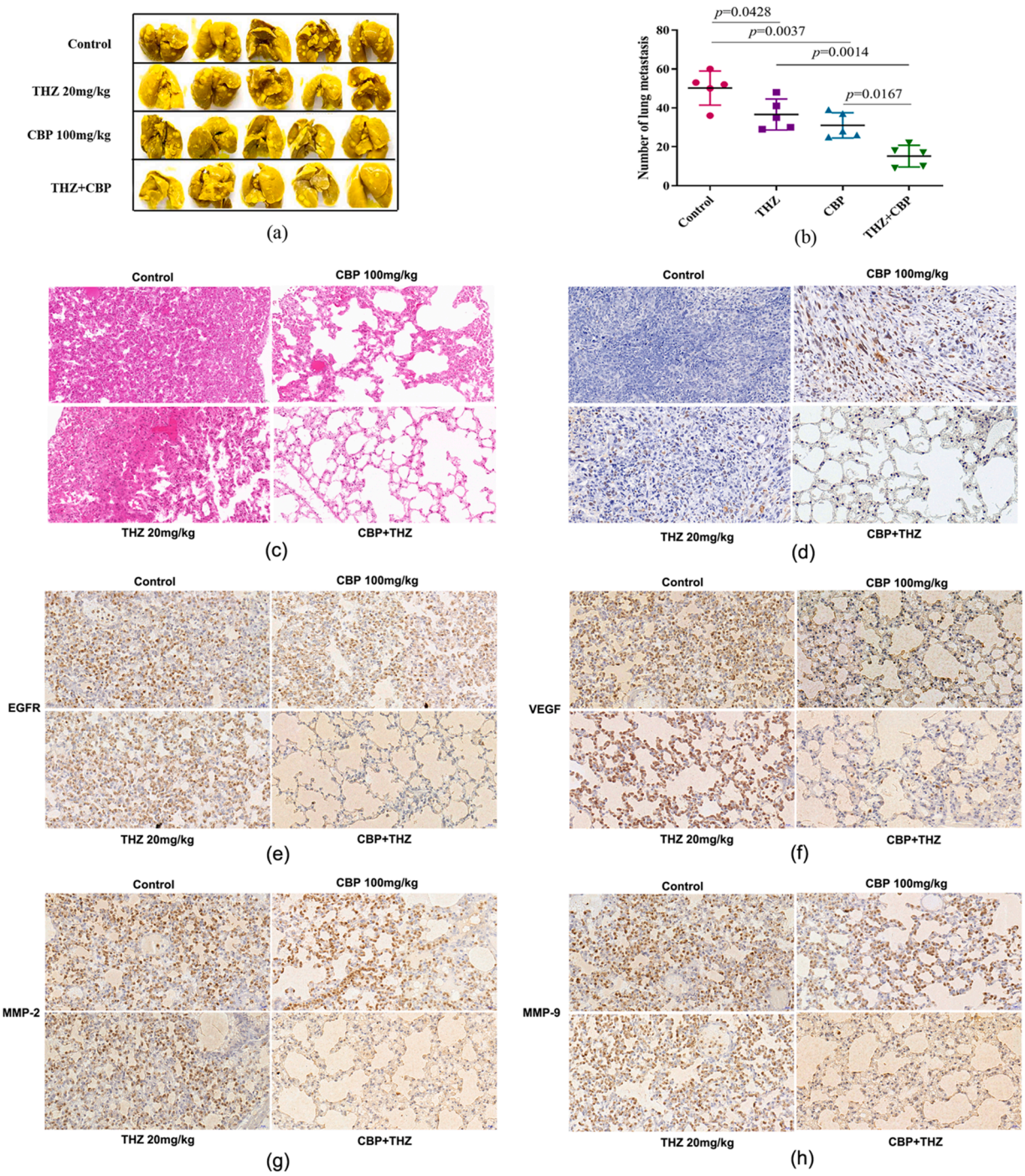

Fig. 5. Combination therapy with THZ and CBP significantly inhibited metastasis in the mouse model of 4T1 pulmonary metastatic tumor. (a) Macroscopic observation of lungs harvested from mice subjected to different treatments as indicated. (b) The number of metastatic nodes. (c, d) H&E and TUNEL staining of lung tissues. (e-h) Immunohistochemistry staining of EGFR, VEGF, MMP2, MMP9 in lung tissues. Magnification: 400 × .

Tumorigenicity of ALDH1^{high} 4T1 cells

ALDH1 (aldehyde dehydrogenase) activity has been widely used as a marker to identify CSCs in various cancers [16–19]. The tumorigenicity of ALDH^{high} and ALDH^{low} 4T1 cells was evaluated by a ALDEFLUOR Kit. The rates of ALDH^{high} and ALDH^{low} cells were 13.6% and 11.6%, respectively (Fig. 7(a)). Equal amounts of ALDH^{high} and ALDH^{low} 4T1 cells were injected into the opposite sides of the same mouse. Tumor development is shown in Fig. 7(b). Mice injected with 50,000 ALDH^{high} and ALDH^{low} cells developed tumors, and the ALDH^{high} cells formed significantly larger tumors than the ALDH^{low} cells. In mice injected only 5,000 or 500 ALDH^{high} and ALDH^{low} cells, only ALDHhigh cells could form large tumors. Our findings indicate that ALDH^{high} CSCs play a significant role in tumorigenesis.

THZ and CBP mono- and combination therapy target 4T1 CSCs in vivo

To confirm the anti-CSC function of THZ in vivo, either alone or with CBP, we investigated the residual 4T1 ALDH^{high} cells in 4T1 tumor tissues harvested from the last treatment. As shown in Fig. 8, 6.2% (6.93 ± 1.19%) of residual ALDH^{high} CSCs were observed in THZ-treated tumors, and in control group is 14.5% (13.77 ± 0.74%). However, CBP

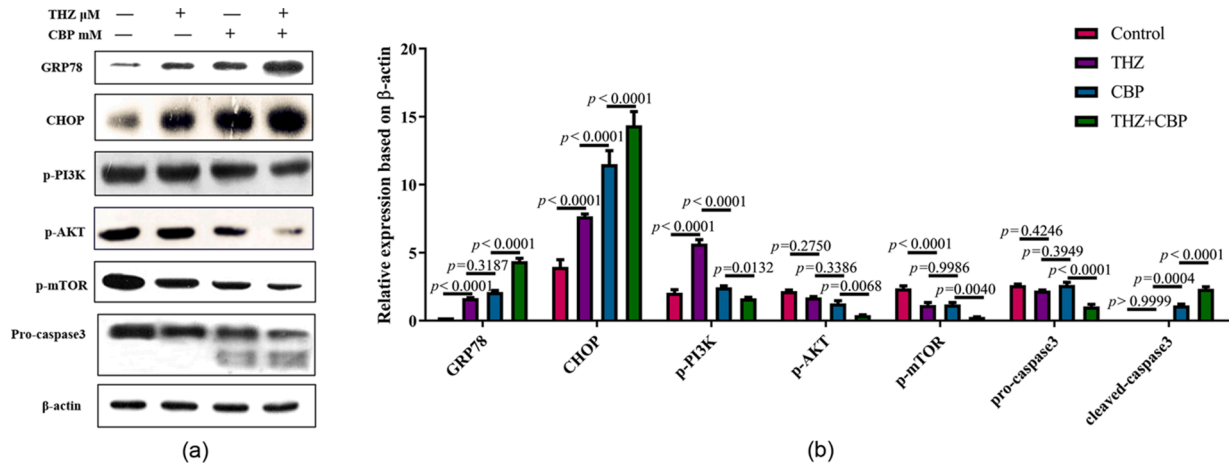

Fig. 6. Combination therapy with THZ and CBP decreased the phosphorylation of major components of the PI3K/mTOR pathway and induced ER stress in vivo. (a) The expression of PI3K/mTOR signaling proteins and ER stress-related proteins in tissues derived from BALB/c mice tumors were determined. (b) Quantitative analysis of (a) ($n = 3$).

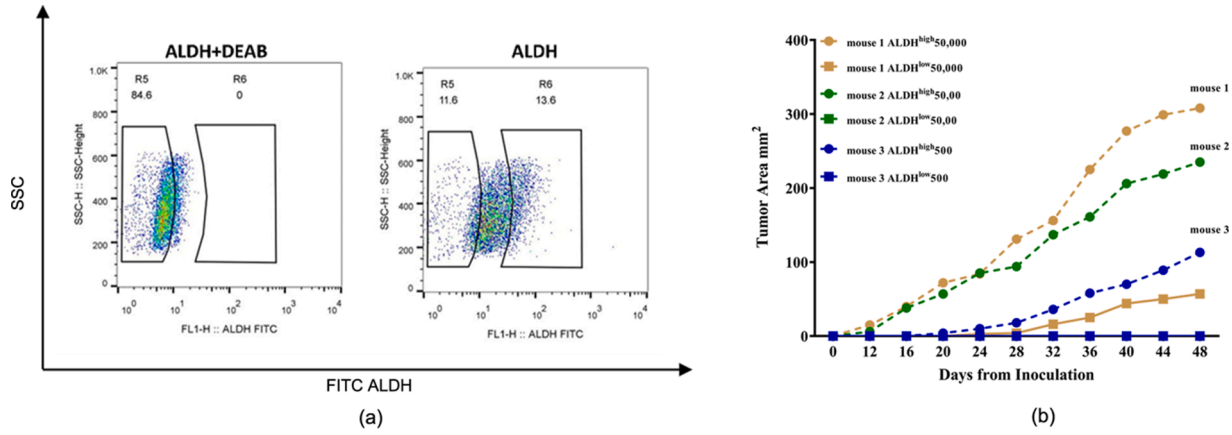

Fig. 7. Testing the tumorigenicity of ALDH^{high} 4T1 cells vs. ALDH^{low} 4T1 cells in Balb/c mice. (a) Representative flow cytometry plot showing the sorting of ALDH^{high} and ALDH^{low} 4T1 cells. (b) Equal numbers of ALDH^{high} and ALDH^{low} 4T1 cells were injected into the opposite side of the same mouse. The growth of tumor cells was then observed.

monotherapy revealed a higher level of residual ALDH^{high} CSCs at 9.2% (8.83 ± 0.95%) in tumor tissues. Finally, in the THZ +CBP group, the percentage of ALDH^{high} cells decreased to 5.6% (4.83 ± 0.97%) in 4T1 tumor tissues (Fig. 8(a) and (b)). Taken together, these results demonstrate that THZ could specifically kill CSCs and further enhance the ability of CBP to kill CSCs in mouse 4T1 BC.

To test the stemness of the residual tumor cells, we transplanted 0.5 million cells isolated from mice treated with CBP alone or in combination with THZ into opposite fat pads of the same mouse. Macroscopic observation of the transplanted mice and the average tumor volume showed smaller tumor formation of residual tumor cells in the THZ +CBP group than in the CBP alone group (Fig. 9(a) and (b)), suggesting that the tumorigenicity of residual tumor cells was inhibited more by combination therapy than by CBP treatment. In conclusion, our results suggest that THZ and CBP combination therapy can not only reduce the number of ALDH^{high} 4T1 CSCs, but also halt their tumorigenicity.

Discussion

TNBC is a extremely aggressive subtype of BC known for its high drug resistance, poor prognosis, lack of clear and effective therapeutic targets [20]. Therefore, combination therapy is preferred to increase clinical therapeutic efficiency. In our study, we explored the effect of the combination of THZ and CBP on the proliferation and apoptosis of metastatic 4T1 cells, and clarified the underlying mechanism. We reported that the combination of THZ and CBP could synergistically inhibit 4T1 cell proliferation and trigger mitochondrial-mediated apoptosis via ER stress and the PI3K/AKT pathway. The PI3K/AKT signaling pathway plays an vital role in regulating the biological behavior of tumor malignancies [21]. Our data suggest that the combination of THZ and CBP suppresses the metastasis of 4T1 BALB/c mice tumors in vivo. Moreover, we showed that THZ could sensitize 4T1 CSCs to CBP treatment both in vivo and in vitro, thereby highlighting its potential role in clinical TNBC treatment.

Platinum-based drugs, including cisplatin, carboplatin, and oxaliplatin are diffusely used for the chemotherapy of various cancers [22, 23]. Treatment with a combination of paclitaxel and carboplatin is the current first-line therapy for advanced TNBC; However, after an initial PCR, the majority of patients with TNBC relapse and develop drug resistance, requiring the urgent development of novel therapeutics.

Thioridazine was discovered as a widely used antipsychotic agent many years ago. As research has progressed, THZ has shown antitumor properties, but it also has some side effects, for example, Aslostovar and colleagues studied 13 patients aged 55 years and older with relapsed or refractory acute myeloid leukemia. Oral THZ was administered at 3 dose levels: 25 mg (n = 6), 50 mg (n = 4), or 100 mg (n = 3) every 6 hours for 21 days, and found that dose-limiting toxicities included grade 3 QTc interval prolongation in 1 patient at 25 mg TDZ and neurological events

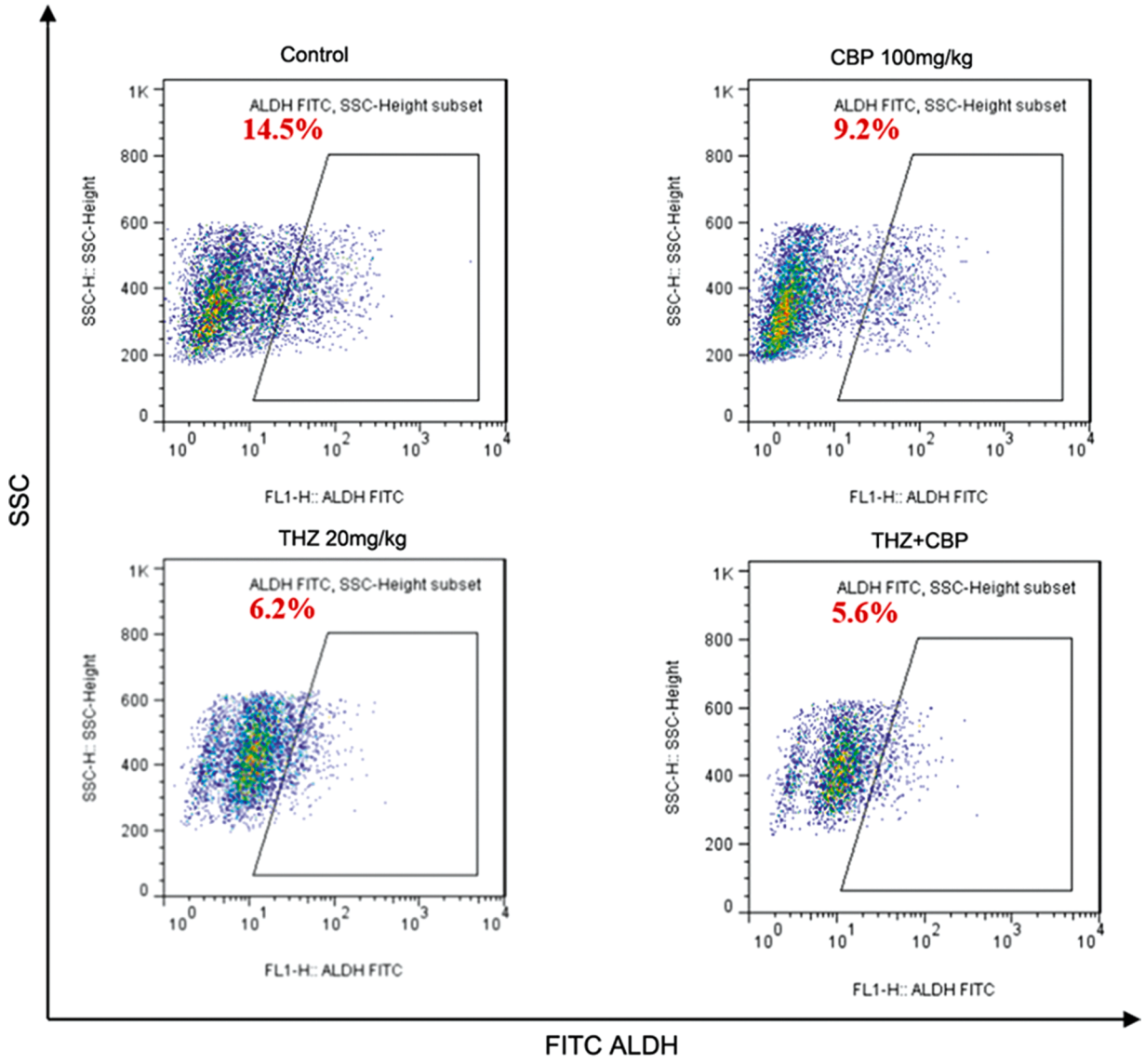

Fig. 8. THZ monotherapy and combination therapy reduced the number of ALDH^{high} 4T1 cancer stem cells. (a) The percentage of ALDH^{high} cells was decreased after treatment with THZ, while the percentage was increased by the administration of CBP. Combination therapy of THZ and CBP significantly reduced the percentage of ALDH^{high} cells in 4T1 tumor issues. (b) The quantitative percentage of ALDH^{high} cells ($n = 5$).

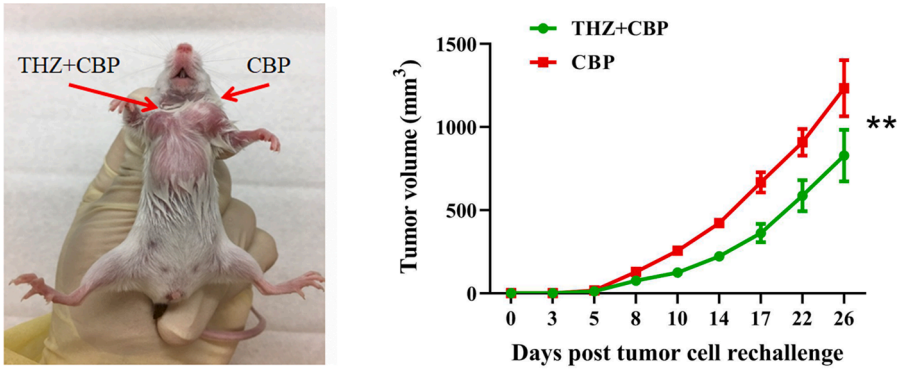

Fig. 9. Tumorigenesis of residual 4T1 cells treated with combination therapy was significantly more reduced than that if cells treated with CBP alone. We transplanted 0.5 million residual 4T1 cells isolated from indicated tumors into opposite fat pads of the same mouse. (a) Macroscopic observation of the tumor size derived from residual cancer stem cells after treatment. (b) The tumor growth after inoculation was measured ($n = 5$).

in 2 patients at 100 mg TDZ (gait disturbance, depressed consciousness, and dizziness) [24]. Another study reported similar results, which found that under proper cardiac evaluation procedures, the use of THZ is safe and does not produce known cardiopathy such as prolongation of QT interval [25]. These preliminary results suggest that THZ represents a potential therapeutic candidates for cancer treatment with acceptable side effects. In a drug screen to identify efficient drugs for targeting CSCs, THZ was first reported to possess strong anti-cancer stem cell properties [9]. Since then, many studies have been devoted to revealing the role of THZ for many cancers, including lung cancer [26,27], colorectal cancer [28,29], gastric cancer [30,31], cervical cancer [32], and BC [33].

The anticancer effect of THZ is mainly through inhibiting cell proliferation, suppressing metastasis, and inducing apoptosis and autophagy, therefore, reversing multidrug resistance. Johannessen et al. reported that THZ induces autophagy and sensitizes glioblastoma cells to temozolomide [34]. In lung and ovarian cancers, THZ showed cytotoxic effects and increased sensitivity to cisplatin in cancer cells [26]. In addition, THZ was shown to suppress the growth of GBM cells and induce cell cycle arrest at G1 phase and cell apoptosis [35]. Consistent with these studies, our results demonstrated that THZ inhibited 4T1 cell proliferation and induced apoptosis. We observed that the expression levels of GRP78 and CHOP was increased in THZ-treated 4T1 cells, suggesting that the occurrence of ER stress was often concomitant with THZ-induced apoptosis. Moreover, the intensity of ER stress was amplified in the combination therapy group, implying that apoptosis might be derived from ER stress. Furthermore, we found that the phenotype observed in THZ-treated cells was characterized by the inhibition of PI3K/AKT/mTOR signaling. Thus, our results indicated that THZ could induce apoptosis of cancer cells, especially stem cells, with accumulated ER stress and inhibition of PI3K/AKT/mTOR signaling. Additionally, recent studies have confirmed that THZ can promote the differentiation of tumor stem cells and deactivate them without affecting normal cells, further indicating that THZ may act as a potent anticancer drug [9,27,36,37].

Tumorigenic CSCs are a critical subpopulation of cells intrinsically resistant to conventional chemotherapy and that have enhanced self-renewal and differentiation potential [38,39]. CSCs are known to contribute to drug resistance and tumor metastasis in de novo tumors or in tissues remaining from chemotherapy [40–44], and cancer relapse after treatment, especially in TNBC, in which CSCs play a vital role in recurrence. Therefore, eliminating CSCs is critical for most cancer therapies. To do so, research has focused on combining conventional therapy with CSC-targeting therapies for the treatment of drug-resistant and metastatic cancers. For example, EGFR-targeted therapy with cetuximab has been found to effectively reduce the number of CSCs in TNBC tumors, and ixabepilone produced therapeutic synergism with cetuximab in basal-like cancers [45]. In osteosarcoma CSCs, autophagy is enhanced; however, this process can be targeted by THZ resulting in CSC death. However, whether THZ could target BC stem cells was largely unknown. Thus, in our study, we proved that THZ could target breast CSCs. The ALDHhigh CSC population was decreased both in vitro and in vivo after THZ monotherapy, and this effect was even more profound when THZ was combined with CBP, which ultimately contributed to suppressed tumorigenicity. These findings indicate that THZ could be acted as an anti-CSC agent in combination therapy for drug-resistant BC cells.

Currently, we have not conduct clinical trials about THZ. As we known, thioridazine (THZ) is a commonly used antipsychotic drug with acceptable side effects; Chang et.al selected 1,631 psychiatric patients ever receiving THZ for more than 30 days within 6 months and paired with 6,256 randomly selected non-THZ controls, and found that the incidence of hyperlipidemia, coronary artery disease and chronic pulmonary disease did not differ between the two groups [46]. However, clinical application of THZ in the treatment of solid tumors is rarely reported. Based on the results of previous cell lines and animal studies, as well as the potential biosafety of THZ in vivo, which suggest THZ is a promising candidate for the treatment of human tumors. Although we have identified the critical synergistic effect of THZ when combined with CBP in 4T1 cells, whether this combination is also effective for other subtypes of BC and cancers warrants additional detailed studies.

Conclusions

In our study, THZ showed a great effect against both BC cells and CSCs in vivo and in vitro via regulation of ER stress and the PI3K/AKT pathway, when combined with CBP therapy. Our study suggests that THZ could act as an efficient drug for targeting and eliminating BC stem cells. These findings provide a framework for subsequent clinical studies aimed at developing methods to suppress tumor metastasis and reduce tumor recurrence. Moreover, THZ has already been approved by the FDA, facilitating its use in cancer therapy. This original combination therapy may be beneficial for the clinical treatment of drug-resistant and metastatic TNBC with high efficacy and low cost.

Data availability

The data used to support the findings of this study are included within the article.

CRediT authorship contribution statement

Yi Wang: Conceptualization, Validation, Investigation, Writing – original draft, Project administration, Funding acquisition. **Leiming Xia:** Methodology, Software, Validation, Project administration, Writing – original draft. **Jing Lin:** Methodology, Formal analysis, Investigation, Writing – original draft. **Li Gong:** Formal analysis, Data curation. **Yang Xia:** Software, Visualization. **Yang Xu:** Software. **Liu Liu:** Validation. **Jian Bao:** Investigation. **Congshu Zhang:** Investigation. **Yuqing Chai:** Resources. **Hongxia Li:** Conceptualization, Writing – review & editing, Supervision, Funding acquisition.

Conflicts of Interest

The authors declare no conflict of interest.

Acknowledgments

This research was funded by High-End Foreign Experts Project (nos. G2021019011L) and the Research Fund Projects of Anhui Institute of Translational Medicine in 2021 (nos. 2021zhyx-C70). The abstract mentioning the presentation of the manuscript similar in abstract we have presented at Association for Cancer Research (AACR) conferences, (Proceedings: AACR Annual Meeting 2020; April 27-28, 2020 and June 22-24, 2020; Philadelphia, PA. Link:“https://cancerres.aacrjournals.org/content/80/16_Supplement/3803"). We sincerely thank Yuanyuan Liu, Wicha Max, Alfred E. Chang and Yangyi Bao for their help in the revision of the abstract at the conference. And thanks to professor Li Qiao for recommending us to attend the AARC conference and presented the abstract. Now we will publish it as an article for the first time.

References

[1] H.Y. Lin, P.Y. Chu, Advances in understanding mitochondrial MicroRNAs (mitomiRs) on the pathogenesis of triple-negative breast cancer (TNBC), Oxid. Med. Cell. Long. 2021 (2021), 5517777.
[2] D. Agostini, V. Natalucci, G. Baldelli, M. De Santi, S. Donati Zeppa, L. Vallorani, G. Annibalini, F. Lucertini, A. Federici, R. Izzo, V. Stocchi, E. Barbieri, New insights into the role of exercise in inhibiting mTOR signaling in triple-negative breast cancer, Oxid. Med. Cell. Long. 2018 (2018), 5896786.
[3] J. Liu, L. Ye, Q. Li, X. Wu, B. Wang, Y. Ouyang, Z. Yuan, J. Li, C. Lin, Synaptopodin-2 suppresses metastasis of triple-negative breast cancer via inhibition of YAP/TAZ activity, J. Pathol. 244 (1) (2018) 71–83.

[4] E. Hernández-SanMiguel, R. Gargini, T. Cejalvo, B. Segura-Collar, P. Núñez-Hervada, R. Hortigüela, J.M. Sepúlveda-Sánchez, A. Hernández-Laín, A. Pérez-Núñez, E. Sanz, P. Sánchez-Gómez, Ocoxin Modulates Cancer Stem Cells and M2 Macrophage Polarization in Glioblastoma, Oxid. Med. Cell. Long. 2019 (2019), 9719730.

[5] Y. Hu, L. Lu, Y. Xia, X. Chen, A.E. Chang, R.E. Hollingsworth, E. Hurt, J. Owen, J. S. Moyer, M.E. Prince, F. Dai, Y. Bao, Y. Wang, J. Whitfield, J.C. Xia, S. Huang, M. S. Wicha, Q. Li, Therapeutic efficacy of cancer stem cell vaccines in the adjuvant setting, Cancer Res. 76 (16) (2016) 4661–4672.

[6] G. Spengler, Á. Csonka, J. Molnár, L. Amaral, The anticancer activity of the old neuroleptic phenothiazine-type drug thioridazine, Anticancer Res. 36 (11) (2016) 5701–5706.

[7] V. Singh, P.K. Jaiswal, I. Ghosh, H.K. Koul, X. Yu, A. De Benedetti, Targeting the TLK1/NEK1 DDR axis with Thioridazine suppresses outgrowth of androgen independent prostate tumors, Int. J. Cancer 145 (4) (2019) 1055–1067.

[8] T. Lang, Y. Liu, Z. Zheng, W. Ran, Y. Zhai, Q. Yin, P. Zhang, Y. Li, Cocktail strategy based on spatio-temporally controlled nano device improves therapy of breast cancer, Adv. Mater. 31 (5) (2019), e1806202.

[9] E. Sachlos, R.M. Risueño, S. Laronde, Z. Shapovalova, J.H. Lee, J. Russell, M. Malig, J.D. McNicol, A. Fiebig-Comyn, M. Graham, M. Levadoux-Martin, J.B. Lee, A. O. Giacomelli, J.A. Hassell, D. Fischer-Russell, M.R. Trus, R. Foley, B. Leber, A. Xenocostas, E.D. Brown, T.J. Collins, M. Bhatia, Identification of drugs including a dopamine receptor antagonist that selectively target cancer stem cells, Cell 149 (6) (2012) 1284–1297.

[10] V. Roy, B.A. Pockaj, J.B. Allred, H. Apsey, D.W. Northfelt, D. Nikcevich, B. Mattar, E.A. Perez, A Phase II trial of docetaxel and carboplatin administered every 2 weeks as preoperative therapy for stage II or III breast cancer: NCCTG study N0338, Am. J. Clin. Oncol. 36 (6) (2013) 540–544.

[11] A. Tutt, H. Tovey, M.C.U. Cheang, S. Kernaghan, L. Kilburn, P. Gazinska, J. Owen, J. Abraham, S. Barrett, P. Barrett-Lee, R. Brown, S. Chan, M. Dowsett, J. M. Flanagan, L. Fox, A. Grigoriadis, A. Gutin, C. Harper-Wynne, M.Q. Hatton, K. A. Hoadley, J. Parikh, P. Parker, C.M. Perou, R. Roylance, V. Shah, A. Shaw, I. E. Smith, K.M. Timms, A.M. Wardley, G. Wilson, C. Gillett, J.S. Lanchbury, A. Ashworth, N. Rahman, M. Harries, P. Ellis, S.E. Pinder, J.M. Bliss, Carboplatin in BRCA1/2-mutated and triple-negative breast cancer BRCAness subgroups: the TNT Trial, Nat. Med. 24 (5) (2018) 628–637.

[12] P. Sharma, S. López-Tarruella, J.A. García-Saenz, C. Ward, C.S. Connor, H. L. Gómez, A. Prat, F. Moreno, Y. Jerez-Gilarranz, A. Barnadas, A.C. Picornell, M. Del Monte-Millán, M. Gonzalez-Rivera, T. Massarrah, B. Pelaez-Lorenzo, M. I. Palomero, R. González Del Val, J. Cortes, H. Fuentes Rivera, D. Bretel Morales, I. Márquez-Rodas, C.M. Perou, J.L. Wagner, J.M. Mammen, M.K. McGinness, J. R. Klemp, A.L. Amin, C.J. Fabian, J. Heldstab, A.K. Godwin, R.A. Jensen, B. F. Kimler, Q.J. Khan, M. Martin, Efficacy of neoadjuvant carboplatin plus docetaxel in triple-negative breast cancer: combined analysis of two cohorts, Clin. Cancer Res. 23 (3) (2017) 649–657.

[13] O. Gluz, U. Nitz, C. Liedtke, M. Christgen, E.M. Grischke, H. Forstbauer, M. Braun, M. Warm, J. Hackmann, C. Uleer, B. Aktas, C. Schumacher, N. Bangemann, C. Lindner, S. Kuemmel, M. Clemens, J. Potenberg, P. Staib, A. Kohls, R. von Schumann, R. Kates, R. Kates, J. Schumacher, R. Wuerstlein, H.H. Kreipe, N. Harbeck, Comparison of neoadjuvant nab-paclitaxel+carboplatin vs nab-paclitaxel+gemcitabine in triple-negative breast cancer: randomized WSG-ADAPT-TN trial results, J. Natl. Cancer Inst. 110 (6) (2018) 628–637.

[14] P. Zhang, Y. Yin, H. Mo, B. Zhang, X. Wang, Q. Li, P. Yuan, J. Wang, S. Zheng, R. Cai, F. Ma, Y. Fan, B. Xu, Better pathologic complete response and relapse-free survival after carboplatin plus paclitaxel compared with epirubicin plus paclitaxel as neoadjuvant chemotherapy for locally advanced triple-negative breast cancer: a randomized phase 2 trial, OncoTargets Ther. 7 (37) (2016) 60647–60656.

[15] H.J. Paholak, N.O. Stevers, H. Chen, J.P. Burnett, M. He, H. Korkaya, S. P. McDermott, Y. Deol, S.G. Clouthier, T. Luther, Q. Li, M.S. Wicha, D. Sun, Elimination of epithelial-like and mesenchymal-like breast cancer stem cells to inhibit metastasis following nanoparticle-mediated photothermal therapy, Biomaterials 104 (2016) 145–157.

[16] D. Vidovic, T.T. Huynh, P. Konda, C. Dean, B.M. Cruickshank, M. Sultan, K. M. Coyle, S. Gujar, P. Marcato, ALDH1A3-regulated long non-coding RNA NRAD1 is a potential novel target for triple-negative breast tumors and cancer stem cells, Cell Death Differ. 27 (1) (2020) 363–378.

[17] S.H. Wang, L. Lu, Y. Fan, M.S. Wicha, Z. Cao, A.E. Chang, J.C. Xia, J.R. Baker Jr., Q. Li, Characterization of a novel transgenic mouse tumor model for targeting HER2+ cancer stem cells, Int. J. Biol. Sci. 10 (1) (2013) 25–32.

[18] W. Chen, S.G. Allen, W. Qian, Z. Peng, S. Han, X. Li, Y. Sun, C. Fournier, L. Bao, R. H.W. Lam, S.D. Merajver, J. Fu, Biophysical phenotyping and modulation of ALDH + inflammatory breast cancer stem-like cells, Small 15 (5) (2019), e1802891.

[19] C. Visus, Y. Wang, A. Lozano-Leon, R.L. Ferris, S. Silver, M.J. Szczepanski, R. E. Brand, C.R. Ferrone, T.L. Whiteside, S. Ferrone, A.B. DeLeo, X. Wang, Targeting ALDH(bright) human carcinoma-initiating cells with ALDH1A1-specific CD8$^+$ T cells, Clin. Cancer Res. 17 (19) (2011) 6174–6184.

[20] S.Y. Hwang, S. Park, Y. Kwon, Recent therapeutic trends and promising targets in triple negative breast cancer, Pharmacol. Ther. 199 (2019) 30–57.

[21] Y. Liu, X. Xu, H. Tang, Y. Pan, B. Hu, G. Huang, Rosmarinic acid inhibits cell proliferation, migration, and invasion and induces apoptosis in human glioma cells, Int. J. Mol. Med. 47 (5) (2021).

[22] H. Kostrhunova, J. Zajac, L. Markova, V. Brabec, J. Kasparkova, A Multi-action Pt (IV) conjugate with oleate and cinnamate ligands targets human epithelial growth factor receptor HER2 in aggressive breast cancer cells, Angew. Chem. Int. Ed. Engl. 59 (47) (2020) 21157–21162.

[23] R.L. Bighetti-Trevisan, L.O. Sousa, R.M. Castilho, L.O. Almeida, Cancer stem cells: powerful targets to improve current anticancer therapeutics, Stem Cells Int. 2019 (2019), 9618065.

[24] L. Aslostovar, A.L. Boyd, M. Almakadi, T.J. Collins, D.P. Leong, R.G. Tirona, R. B. Kim, J.A. Julian, A. Xenocostas, B. Leber, M.N. Levine, R. Foley, M. Bhatia, A phase 1 trial evaluating thioridazine in combination with cytarabine in patients with acute myeloid leukemia, Blood Adv. 2 (15) (2018) 1935–1945.

[25] L. Amaral, J. Molnar, Why and how the old neuroleptic thioridazine cures the XDR-TB patient, Pharmaceuticals (Basel) 5 (9) (2012) 1021–1031.

[26] G. Qian, L. Dai, T. Yu, Thioridazine sensitizes cisplatin against chemoresistant human lung and ovary cancer cells, DNA Cell Biol. 38 (7) (2019) 718–724.

[27] J. Shen, B. Ma, X. Zhang, X. Sun, J. Han, Y. Wang, L. Chu, H. Xu, Y. Yang, Thioridazine has potent antitumor effects on lung cancer stem-like cells, Oncol. Lett. 13 (3) (2017) 1563–1568.

[28] C. Zhang, P. Gong, P. Liu, N. Zhou, Y. Zhou, Y. Wang, Thioridazine elicits potent antitumor effects in colorectal cancer stem cells, Oncol. Rep. 37 (2) (2017) 1168–1174.

[29] X. Lin, J. Zhang, X. Wang, G. Lin, T. Chen, Pre-activation with TLR7 in combination with thioridazine and loratadine promotes tumoricidal T-cell activity in colorectal cancer, Anticancer Drugs 31 (10) (2020) 989–996.

[30] J. Mu, H. Xu, Y. Yang, W. Huang, J. Xiao, M. Li, Z. Tan, Q. Ding, L. Zhang, J. Lu, X. Wu, Y. Liu, Thioridazine, an antipsychotic drug, elicits potent antitumor effects in gastric cancer, Oncol. Rep. 31 (5) (2014) 2107–2114.

[31] J. Mu, W. Huang, Z. Tan, M. Li, L. Zhang, Q. Ding, X. Wu, J. Lu, Y. Liu, Q. Dong, H. Xu, Dopamine receptor D2 is correlated with gastric cancer prognosis, Oncol. Lett. 13 (3) (2017) 1223–1227.

[32] S. Kang, S.M. Dong, B.R. Kim, M.S. Park, B. Trink, H.J. Byun, S.B. Rho, Thioridazine induces apoptosis by targeting the PI3K/Akt/mTOR pathway in cervical and endometrial cancer cells, Apoptosis 17 (9) (2012) 989–997.

[33] M. Tegowski, C. Fan, A.S. Baldwin, Thioridazine inhibits self-renewal in breast cancer cells via DRD2-dependent STAT3 inhibition, but induces a G(1) arrest independent of DRD2, J. Biol. Chem. 293 (41) (2018) 15977–15990.

[34] T.C. Johannessen, M.M. Hasan-Olive, H. Zhu, O. Denisova, A. Grudic, M.A. Latif, H. Saed, J.K. Varughese, G.V. Røsland, N. Yang, T. Sundstrøm, A. Nordal, K. J. Tronstad, J. Wang, M. Lund-Johansen, A. Simonsen, B. Janji, J. Westermarck, R. Bjerkvig, L. Prestegarden, Thioridazine inhibits autophagy and sensitizes glioblastoma cells to temozolomide, Int. J. Cancer 144 (7) (2019) 1735–1745.

[35] C.W. Chu, H.J. Ko, C.H. Chou, T.S. Cheng, H.W. Cheng, Y.H. Liang, Y.L. Lai, C. Y. Lin, C. Wang, J.K. Loh, J.T. Cheng, S.J. Chiou, C.L. Su, C.F. Huang, Y.R. Hong, Thioridazine enhances P62-mediated autophagy and apoptosis through Wnt/β-catenin signaling pathway in glioma cells, Int. J. Mol. Sci. 20 (3) (2019).

[36] H. Yue, D. Huang, L. Qin, Z. Zheng, L. Hua, G. Wang, J. Huang, H. Huang, Targeting lung cancer stem cells with antipsychological drug thioridazine, Biomed. Res. Int. 2016 (2016), 6709828.

[37] O. Camuzard, M.C. Trojani, S. Santucci-Darmanin, S. Pagnotta, V. Breuil, G. F. Carle, V. Pierrefite-Carle, Autophagy in osteosarcoma cancer stem cells is critical process which can be targeted by the antipsychotic drug thioridazine, Cancers 12 (12) (2020).

[38] T. Tanei, K. Morimoto, K. Shimazu, S.J. Kim, Y. Tanji, T. Taguchi, Y. Tamaki, S. Noguchi, Association of breast cancer stem cells identified by aldehyde dehydrogenase 1 expression with resistance to sequential Paclitaxel and epirubicin-based chemotherapy for breast cancers, Clin. Cancer Res. 15 (12) (2009) 4234–4241.

[39] M. Najafi, K. Mortezaee, J. Majidpoor, Cancer stem cell (CSC) resistance drivers, Life Sci. 234 (2019), 116781.

[40] S. Wang, Z. Mou, Y. Ma, J. Li, J. Li, X. Ji, K. Wu, L. Li, W. Lu, T. Zhou, Dopamine enhances the response of sunitinib in the treatment of drug-resistant breast cancer: Involvement of eradicating cancer stem-like cells, Biochem. Pharmacol. 95 (2) (2015) 98–109.

[41] A.S. Cazet, M.N. Hui, B.L. Elsworth, S.Z. Wu, D. Roden, C.L. Chan, J.N. Skhinas, R. Collot, J. Yang, K. Harvey, M.Z. Johan, C. Cooper, R. Nair, D. Herrmann, A. McFarland, N. Deng, M. Ruiz-Borrego, F. Rojo, J.M. Trigo, S. Bezares, R. Caballero, E. Lim, P. Timpson, S. O'Toole, D.N. Watkins, T.R. Cox, M.S. Samuel, M. Martín, A. Swarbrick, Targeting stromal remodeling and cancer stem cell plasticity overcomes chemoresistance in triple negative breast cancer, Nat. Commun. 9 (1) (2018) 2897.

[42] S. Shen, X. Xu, S. Lin, Y. Zhang, H. Liu, C. Zhang, R. Mo, A nanotherapeutic strategy to overcome chemotherapeutic resistance of cancer stem-like cells, Nat. Nanotechnol. 16 (1) (2021) 104–113.

[43] S.Q. Geng, A.T. Alexandrou, J.J. Li, Breast cancer stem cells: Multiple capacities in tumor metastasis, Cancer Lett. 349 (1) (2014) 1–7.

[44] S.R. Sirkisoon, R.L. Carpenter, T. Rimkus, D. Doheny, D. Zhu, N.R. Aguayo, F. Xing, M. Chan, J. Ruiz, L.J. Metheny-Barlow, R. Strowd, J. Lin, A.T. Regua, A. Arrigo, M. Anguelov, B. Pasche, W. Debinski, K. Watabe, H.W. Lo, TGLI1 transcription factor mediates breast cancer brain metastasis via activating metastasis-initiating cancer stem cells and astrocytes in the tumor microenvironment, Oncogene 39 (1) (2020) 64–78.

[45] T. Tanei, D.S. Choi, A.A. Rodriguez, D.H. Liang, L. Dobrolecki, M. Ghosh, M. D. Landis, J.C. Chang, Antitumor activity of Cetuximab in combination with Ixabepilone on triple negative breast cancer stem cells, Breast Cancer Res. 18 (1) (2016) 6.

[46] C.C. Chang, M.H. Hsieh, J.Y. Wang, N.Y. Chiu, Y.H. Wang, J.Y. Chiou, H.H. Huang, P.C. Ju, Association between thioridazine use and cancer risk in adult patients with schizophrenia-a population-based study, Psychiatry Investig 15 (11) (2018) 1064–1070.